POLYPYRROLE/LANTHANUM MANGANITE: A COMPARATIVE STUDY OF MORPHOLOGY, STRUCTURAL, VSM, AND EPR STUDIES

Abstract

Our research focuses on an innovative category of materials achieved through the modification of the conducting polymer Polypyrrole (PPy: Host) with Perovskite compounds (La0.7Ca0.3MnO3 and La0.7Ba0.3MnO3: Doped). This novel material class is tailored to exhibit distinctive properties. Our study delves into the synthesis of these composite materials through the in-situ chemical oxidation method, coupled with an in-depth investigation of their characteristics. Using various analytical techniques, we explored the morphology, chemical composition, crystal phase, and magnetic behavior of these composites. Scanning Electron Microscopy (SEM) revealed their spherical structure, while Energy Dispersive X-ray (EDAX) analysis confirmed the presence of the respective elements. X-ray Diffraction (XRD) highlighted their Orthorhombic phase, while Vibrating Sample Magnetometry (VSM) demonstrated paramagnetic behavior. Additionally, Electron Paramagnetic Resonance (EPR) revealed intriguing interactions between the host and the doped materials, all of which were observed at room temperature.This comprehensive study enhances our understanding of the fundamental interactions between host and doped materials. Moreover, the findings pave the way for potential future applications, such as energy harvesting and Superconducting Quantum Interference Devices (SQUIDs), suggesting exciting prospects for these nanocomposites in emerging technologies.

Keywords: Polypyrrole, Morphology, VSM, EPR.

Authors

Dr. Smitha M. G
Department of Physics
RNS Institute of Technology
Bengaluru, Karnataka, India.
smithamgrao@gmail.com

Shwetha
Department of Electrical and Electronics
RNS Institute of Technology
Bengaluru, Karnataka, India.

I. INTRODUCTION

Conducting polymers represent a category of organic polymers endowed with the ability to conduct electricity. Several notable examples of these polymers have been invented, including polythiophene (PT), polyacetylene (PA), polypyrrole (PPy), and polyaniline (PANi). The presence of conjugated double bonds along the polymer backbone underlies the transport properties characteristic of conducting polymers **[1-3].** By means of a process known as doping, the conductivity of organic polymers can be finely tuned, transitioning the material from insulating to semiconducting. Since the inception of the "Green technology" concept, conducting polymers have captivated researchers' attention, yielding continuous advancements in their properties. These polymers are garnering widespread interest and ongoing refinements in their attributes, contributing to the evolution of cutting-edge devices like OLEDs, organic photodiodes, organic phototransistors, and Squids **[4-6].**

Meanwhile, perovskite, a distinctive category of magnetic material, has captured considerable interest within the research community due to its potential applications as a capacitor, sensor, and memory device. The perovskite family encompasses various types characterized by the general formula ABO3. In this formula, 'A' represents an alkali metal or lanthanide (cation (divalent)) with a larger ionic radius, while 'B' stands for a cation (tetravalent) with a smaller ionic radius, typically a 3d or 5d transitional metal ion. The 'A' atom occupies the corner lattice positions, the 'B' atom takes up the central lattice position, and the 'O' atoms are positioned at the face center lattice. The selection of ions for the A and B lattice positions is outlined in a branched structure, depicted in figure 1. The perovskite oxides with the composition R1-xAxO3, where R (La, Nd, Pr, Y, etc.) signifies a rare earth ion and A represents an alkali or alkaline cation (Ca2+, Sr2+, Ba2+, Na2+, K2+), belong to the family known as mixed valence manganites. This nomenclature is rooted in the fact that these materials encompass manganese (Mn) ions in diverse valence states. The transport and magnetic properties of these materials predominantly arise from the mixed valence state of manganese **[7,8].**

Among various combinations of magnetic materials, lanthanum manganite stands out due to its remarkable property known as colossal magnetoresistance. This material exhibits a transition between ferromagnetic and paramagnetic states in response to changes in a magnetic field. Such variations in magnetic fields are crucial for specific applications, notably in devices like SQUIDs.

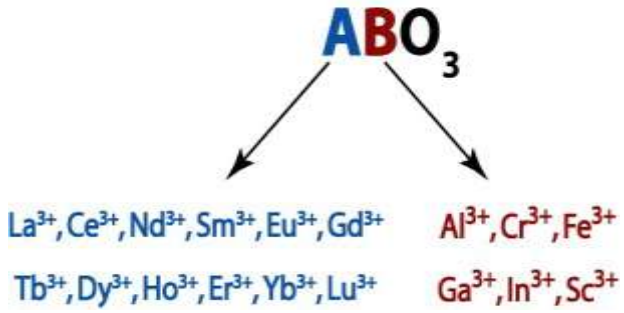

Figure 1: Choice of A-Site and B-Site Elements

It is widely anticipated that organic-inorganic composites will play a pivotal role in advancing advanced functional nanomaterials. The exploration of these materials is a collaborative effort among material scientists, physicists, chemists, and biologists, all working to harness the potential for creating smart materials that can benefit the inorganic, organic, and biological domains. These polymer composite materials hold promise across various applications, including electronics, environmental solutions, optics, photovoltaics, fuel cells, sensors, smart microelectronics, SQUIDs, and even nano ceramic-polymer integration in the automotive industry **[9-13].**

For our current research, we've chosen polypyrrole as the host material and employed La0.7Ca0.3MnO3 and La0.7Ba0.3MnO3 nanoparticles as dopants. Our focus has been on comprehensively studying the morphology, crystalline phases, and magnetic behavior of these composite materials.

II. APPARATUS USED FOR THE STUDY

1. **SEM:** Vega3 TESCAN, and Leica Stereo scan-440 equipped with a Phoenix are used to study the morphology and energy dispersive analysis of X-rays (EDAX).

2. **XRD:** XPERT-3, operating at a voltage of 45 kV and a current of 30 mA with Cu kα radiation has been employed to analyze the shape and size of the compounds.

3. **VSM:** Lake Shore Cryotronics, USA 7400-S series vibrational frequency at 85 Hz is used.

4. **EPR:** JEOL Model JES FA200 EPR instrument at room temperature.

III. SYNTHESIS OF THE COMPOUND

1. **Synthesis of Conducting Polymer Polypyrrole:** The synthesis of Polypyrrole is achieved through an in situ chemical oxidation method as follows:

   First, we prepare a solution by dissolving 0.2 M of the monomer pyrrole in 100 ml of distilled water. We place the beaker containing this pyrrole solution on a magnetic stirrer, stirring at 500 rpm. To maintain a temperature of 0°C-5°C, use a tray filled with ice pellets around the beaker. Next, We prepare the oxidizing agent solution using Ammonium per sulfate (APS): 0.6 M (13.6 g) dissolved in 100 ml of distilled water. Gradually added the APS solution drop by drop to the pyrrole solution in the beaker, allowing the reaction to proceed for 5 hours. After the reaction, We filter the solution to separate the precipitate.

   The precipitate is placed it in a hot air oven at 100°C for approximately 2 hours until a dry compound is obtained. Once the compound is dry, we grind or mortar it to obtain a fine powder it is then weighed and the sample is stored for further studies.

2. **Synthesis of LCM and LBM Nanoparticle:** LCM and LBM nanoparticle were synthesized by the Sol-Gel Method. For the synthesis, the chemicals La_2O_3, $CaCO_3$, $MnCO_3$ (for LCM) and La_2O_3, $BaCO_3$, and $MnCO_3$ for (LBM) (Sigma-Aldrich: 99%) are

taken in a Stoichiometric ratio. The solution LCM manganite is made by dissolving La_2O_3, $CaCO_3$, $MnCO_3$ with 20 ml of nitric acid and 10 ml of water. Similarly, The solution LBM manganite is made by dissolving La_2O_3, $BaCO_3$, $MnCO_3$ with 20 ml of nitric acid and 10 ml of water in separate beakers. The solutions are Stirred well till the chemicals dissolve completely. A polymer precursor polyethylene glycol measuring 30 ml is added separately to both beakers containing LCM and LBM solutions. The mixture is kept on a hot plate and heated to 100 ºC initially and then increased to 250 °C to clear out the volatile compound. It is finally sintered in a Muffle Furnace to 1000 °C for 5 h for LCM and 7 h to get the LBM nano powder. The samples ae weighed and stored for further studies.

3. **Synthesis of Ppy/LCM and Ppy/LBM Nanocomposites:** The composites of PPy/LCM and PPy/LBM were synthesized by chemical oxidation method. To prepare the composite PPy/LCM 10, 10 % (PPy weight) of the weight of LCM is taken and added to pyrrole (The molar ratio of pyrrole taken is similar to the one explained in section A). APS solution (Molar ratio is taken as similar to the one explained in section A) taken in a burette is added dropwise to the mixture of PPy and LCM. The experimental procedure is followed as explained in section A. This sample gives PPy-LCM10 nanocomposite. Similarly, the other composites of PPy/LCM were synthesized by adding 20%, 30%, and 40% weight percent of LCM to the pyrrole solution.

   Similar procedure is followed to get PPy/LBM 10. Further to get other composites of PPy/LBM by adding 20%, 30%, and 40% weight percent of LBM to pyrrole and repeating the above said method.

IV. CHARACTERIZATION STUDIES

1. SEM Analysis

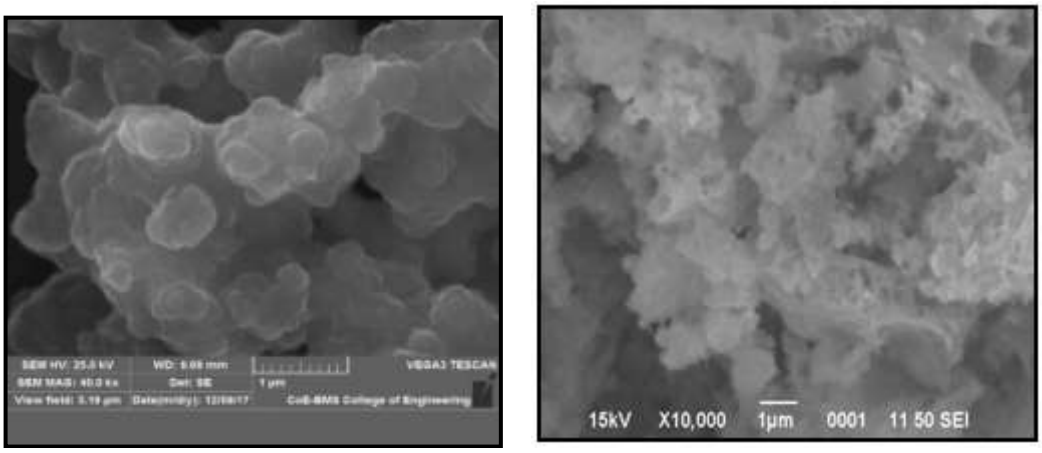

Figure 2: a: Pure Ppy **b:** Pure LCM

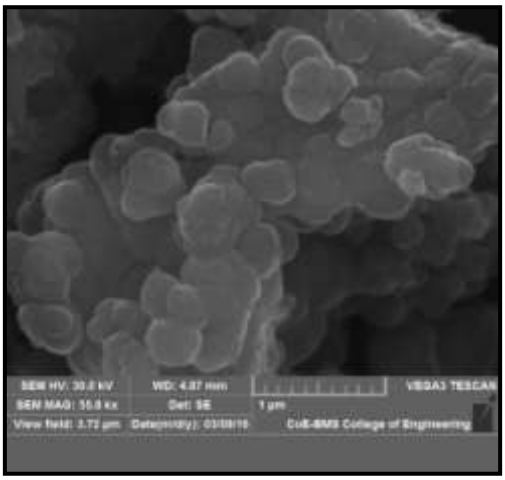

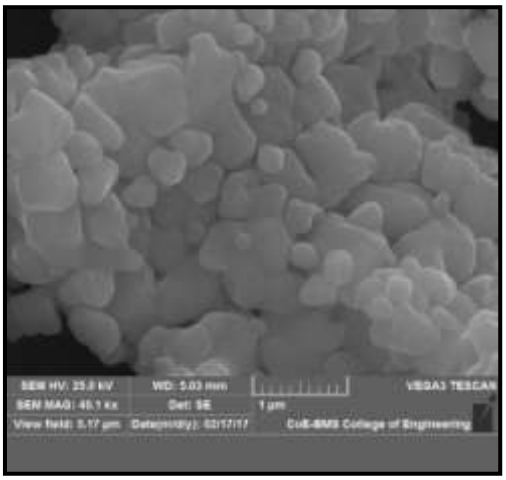

c: PPy-LCM50 **d:** Pure LBM

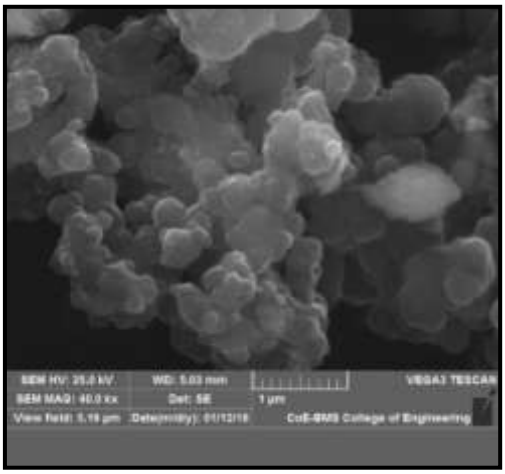

e: PPy-LBM50

The SEM images provide valuable insights into the microstructure of the materials studied:

- The SEM image of pure PPy (Figure 2.a) illustrates a compacted globular structure **[14].**
- In the image of LCM (Figure 2.b), the presence of LCM suggests agglomerated nanoparticle formation.
- The images of PPy/LCM 50 composites (Figure 2.c) reveal a globular structure with embedded LCM nanoparticles within the polypyrrole matrix. The presence of LCM in PPy forms clustered regions, leading to a reduction in the length of the PPy chains.
- The morphological image of LBM (Fig 2.d) displays a spherical structure **[15].**
- In contrast, the composites of PPy/LBM 50 (Figure 2.e) exhibit a globular structure embedded with LBM nanoparticles within the polypyrrole matrix. LBM nanoparticles form a more clustered network with the PPy chain, further reducing the length of the PPy chains.

- These SEM observations provide valuable information about the morphology and distribution of nanoparticles within the polymer matrix, which is crucial for understanding the properties and behavior of these materials.

2. **XRD Analysis:** X-ray diffraction is employed for the identification of the crystalline phases within prepared samples. The X-rays are generated utilizing Cu K-alpha radiation with a wavelength of 1.54 Å. The data is collected in a slow scan mode, systematically covering the 2θ angle range from 10° to 80° with 0.030° increments. The average crystallite size of the particles is subsequently determined using the Scherrer equation.

$$D = \frac{K\lambda}{\beta \cos\theta} \quad \text{..... (1)}$$

Where D, β, θ are crystallitte size (nm), full width at half maximum (degrees) and Bragg angle (degrees) respectively, K= 0.9 and λ = 1.54 Å.

In the present work , the crystalline phase of Pure PPy, pure LCM, PPy/LCM nano composites, and pure LBM and PPy/LBM naocomposites are studied.

The X-ray diffraction (XRD) pattern of PPy is depicted in Figure 3.a, indicating the amorphous character of PPy, with a broad peak centered around 26° [175]. Figures 3.b and 3.c showcase the XRD patterns of Pure LCM and Pure LBM respectively. For Pure LCM, distinct reflection planes appear at (1 01), (0 0 2), (0 2 2), (0 4 0), (0 4 2), (4 0 0), (3 0 3), and (1 6 1), corresponding to peaks located at 21.6°, 32°, 40°, 46.2°, 57°, 69.6°, 71.9°, and 78.8°. Reference to the JCPDS card no: 49-416 confirms the orthorhombic crystal phase of LCM with the Pnma space group **[14].** Turning to Pure LBM, its Bragg's reflection planes are denoted as (0 2 0), (1 2 1), (2 2 0), (0 4 0), (2 2 2), and (2 4 2), corresponding to peaks at 22.5°, 32.5°, 40°, 46.5°, 58°, and 68°, aligning with data from JCPDS file 89-569 (no 74). The crystalline phase of LBM nanoparticles is confirmed as orthorhombic, described by the lmma space group **[16].**

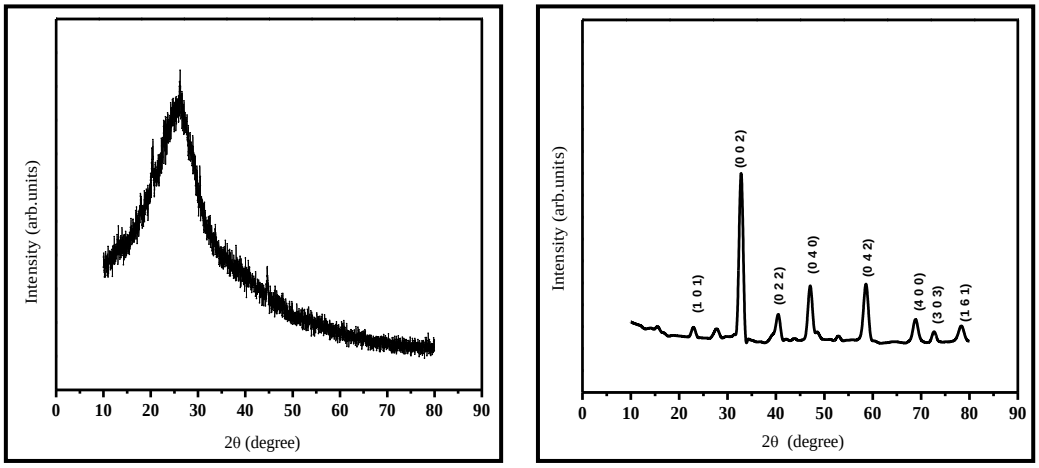

Figure 3: a: Pure PPy **b:** Pure LCM

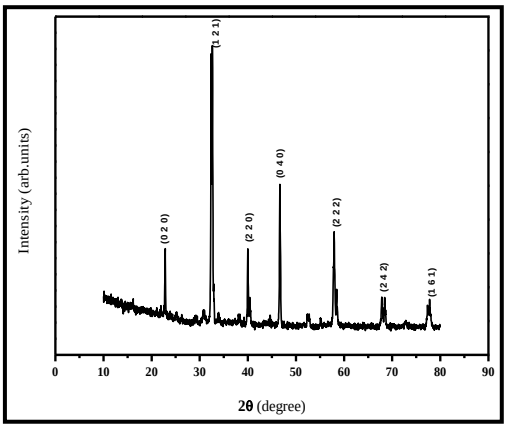

c: Pure LBM

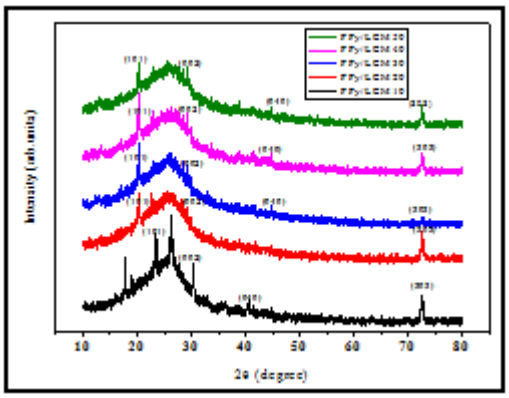

d: Ppy/LCM Nano Composites

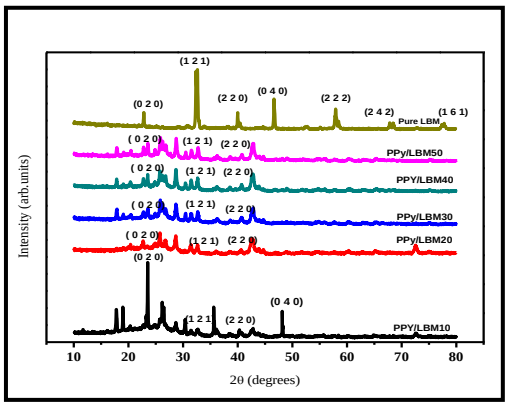

e: Ppy/LBM Nano Composites

In Figure 3.d, the XRD pattern of PPy/LCM nanocomposites is presented. The graphs reveal the polycrystalline nature of the composites, as evidenced by the peak shift to lower angles and a corresponding reduction in peak intensity. This phenomenon is attributed to unique orientation effects seen exclusively in layered compounds and the presence of stacking defects. Notably, several of the dominant peaks observed in Fig 3.d are not discernible in the XRD pattern of PPy/LCM nanocomposites. The phenomenon is termed XRD amorphous, observed in composites where the dopant crystallite size falls below the XRD instrument's detection threshold. Additionally, the absence of specific peaks within these composites is linked to their multiphase formation or potentially due to particles not aligning along the plane of X-ray incidence. The shift in peak positions is a result of thermal expansion caused by internal strain stemming from differing particle sizes between PPy (micrometers) and LCM (nanometers). The

Figure 3.e showcases the XRD pattern of PPy/LBM nanocompounds. Similar to PPy/LCM composites, the graph of PPy/LBM reveals the polycrystalline nature of the composites, with peak shifts towards lower angles and corresponding peak height reductions. This outcome is linked to orientation effects and stacking defects. Notably, certain significant peaks evident in figure 3.4.e are absent in the XRD pattern of PPy/LBM nanocomposites. The non-appearance of these peaks can be ascribed to the

multiphase nature of the composites. The observed shift in peak positions towards lower angles is attributed to the thermal expansion of the composites, arising from internal strain due to particle size discrepancies **[17].**

3. **VSM Measurement of Ppy/LCM Nano Compound:** The magnetic properties of PPy/LCM compound samples were examined, and the plots illustrating magnetic moment versus the applied magnetic field for these composites are displayed in figures 4.(a-e).

In Figures 5.3(a-k) depicting PPy/LCM and PPy/LBM nano compounds, a paramagnetic nature is observed at room temperature. This behavior is ascribed to the random substitution positions of dopants, causing local disruptions in the host material due to spin-orbit coupling. It's also noteworthy that intrinsic changes influence variations in the coercive field, leading to a reduction in anisotropy energy. These factors collectively contribute to the incidental fluctuation of energy associated with the movement of domain walls when interacting with the imperfect structure of the material **[18-24]**.

As indicated in table 5.1, it is observed that the saturation magnetization consistently decreases with increasing doping concentration for PPy/LCM. However, for PPy/LBM nano composites, saturation magnetization decreases for PPy/LBM10 and PPy/LBM20, but then increases for PPy/LBM30, PPy/LBM40, and PPy/LBM50. The decrease in magnetization is attributed to the random substitution positions of dopants within the PPy chain. The subsequent increase in magnetization beyond PPy/LBM30 is attributed to an effective enhancement in the local polarization of the polymer's polarons. The following plot shows the variation of Magnetic moment with a Magnetic field at room temperature.

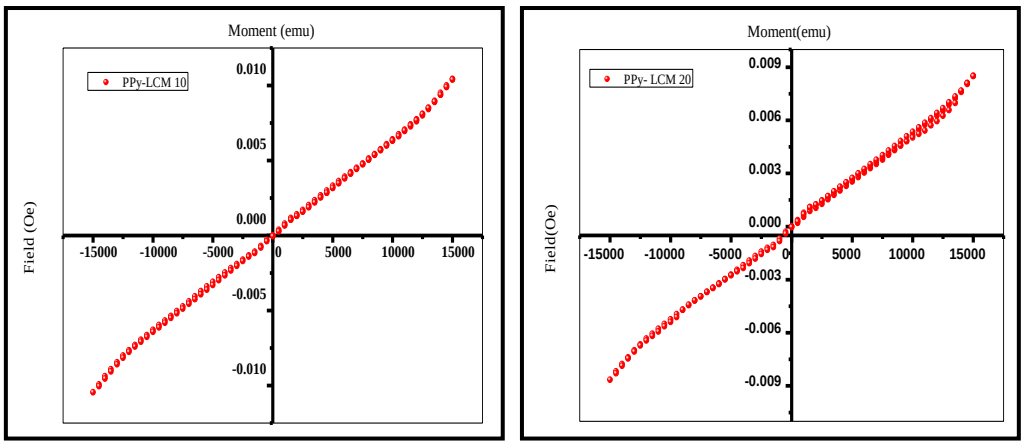

Figure 4: a: PPy/LCM 10 **b:** PPy/LCM 20

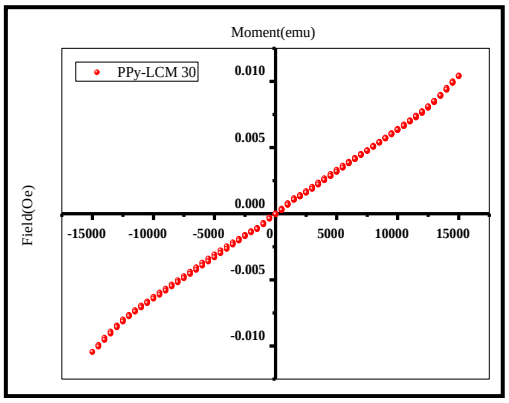

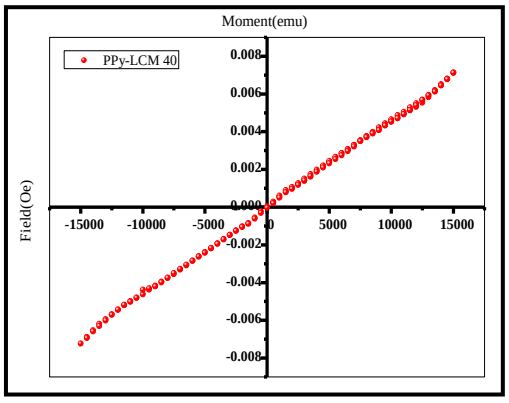

c: PPy/LCM 30 **d:** PPy/LCM 40

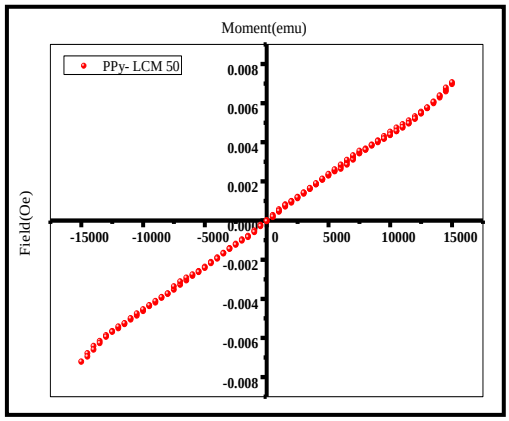

e: PPy/LCM 50

4. **VSM Measurement of Ppy/LBM Nano Compound:** The samples of PPy/LBM nano compound were analyzed for their magnetic properties, the plot of magnetic moment versus the field for the composites is shown in Figure 4(f-j).

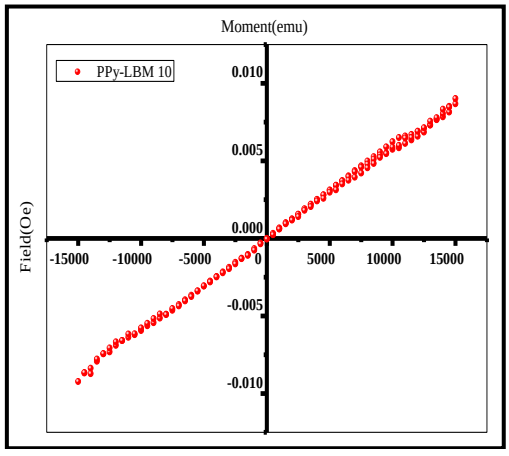

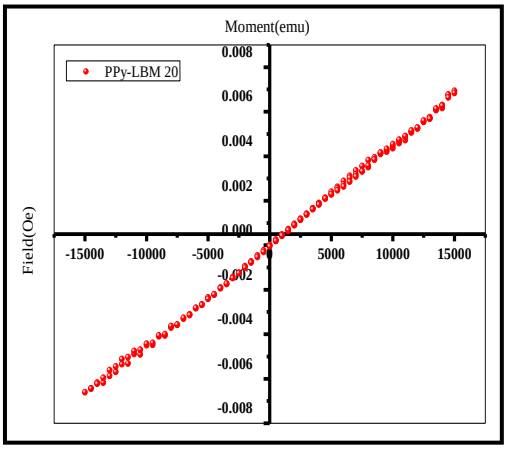

Figure 4: f: PPy/LBM 10 **g:** PPy/LBM 20

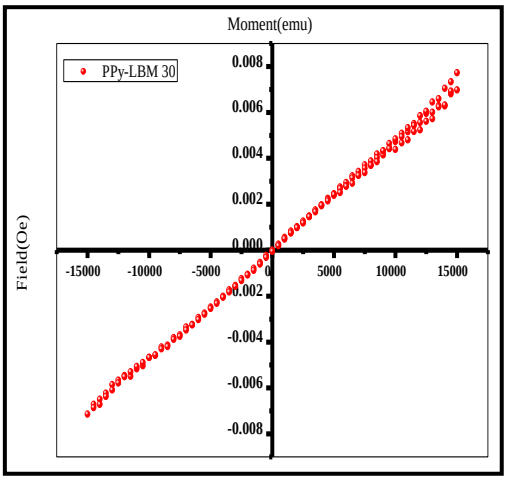

h: PPy/LBM 30

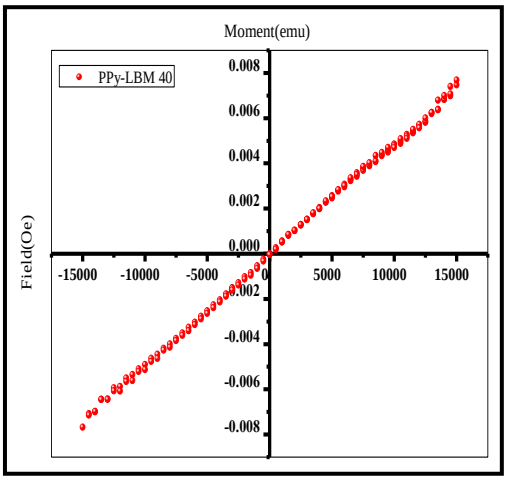

i: PPy/LBM 40

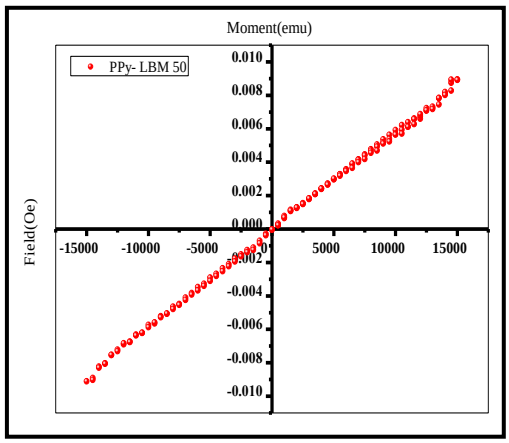

j: PPy/ LBM 50

The intensity of magnetization, coercivity, and retentivity of the samples are listed in the table 1.

Table 1: Intensity of Magnetization, Coercivity, and Retentivity of the Ppy/LCM and Ppy/LBM Nano Compounds

Name of the Compound	Magnetization M_s $x10^{-3}$ (emu/g)	Coercivity Hc (Oe)	Retentivity M_r $x10^{-6}$(emu)
PPy/LCM10	10.44	44.44	27.915
PPy/LCM20	8.582	31.517	19.901
PPy/LCM30	7.6452	47.457	22.025
PPy/LCM40	7.1841	44.331	21.211
PPy/LCM50	7.1321	45.221	20.721
PPy/LBM10	9.125	36.583	19.92
PPy/LBM20	6.7685	62.594	30.717
PPY/LBM30	7.42	53.847	26.250

PPy/LBM40	7.6827	41.403	20.618
PPy/LBM50	9.029	7.8905	1.9538

5. **Electron Paramagnetic Resonance (EPR) Studies:** Electron paramagnetic resonance (EPR), also known as electron spin resonance (ESR), serves as a valuable tool for comprehending the interaction between unpaired electrons and the host material. At its core, this technique revolves around exciting electron spins. EPR spectroscopy is particularly well-suited for unraveling the interplay between electrons and organic compounds containing free radicals, as well as transition metal ions and defects. Uniquely, this method precisely detects unpaired electrons, offering exceptional capability in categorizing paramagnetic substances due to their pronounced sensitivity to local surroundings. EPR spectrum of PPy/LCM nano compound

   The following Figure 5 (a-e) shows the EPR spectrum of the PPy/LCM nano compound.

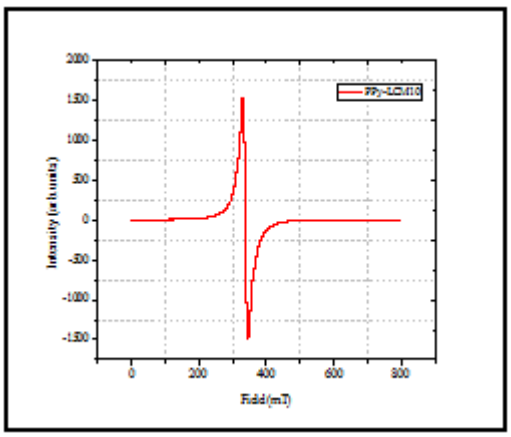

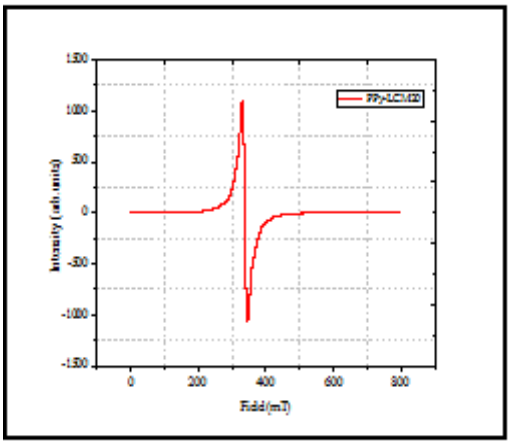

Figure 5: a: PPy/LCM 10 **b:** PPy/LCM 20

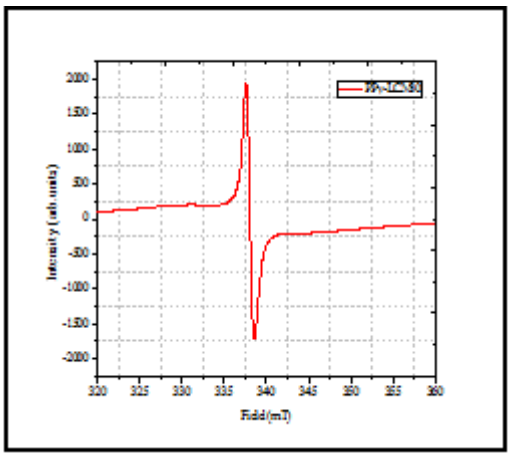

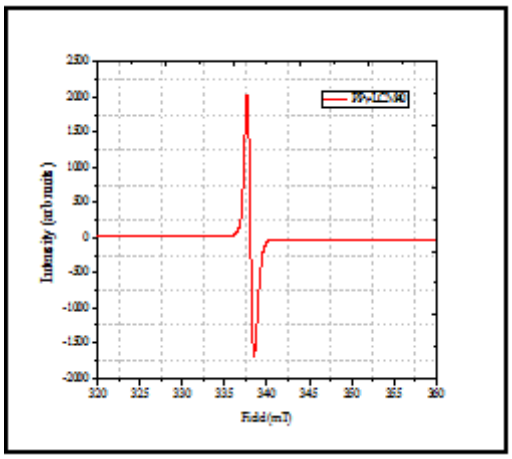

c: PPy/LCM 30 **d:** PPy/LCM 40

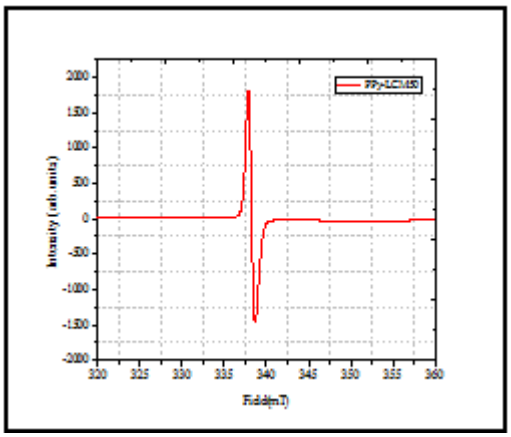

e: PPy/LCM 50

6. **EPR Spectrum of Ppy/LBM Nano Compound:** The following figures 5. (f-j) shows the EPR spectrum of PPy/LBM nano compound.

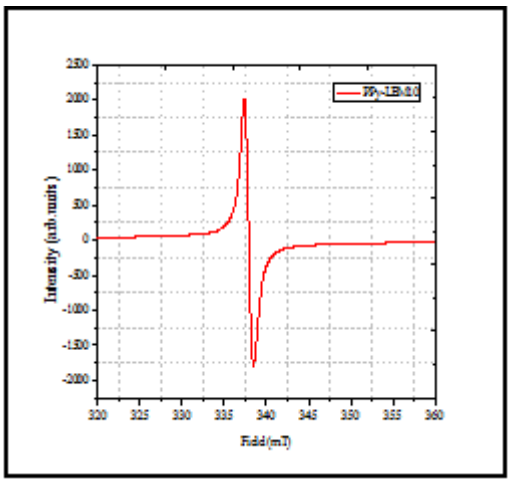

Figure 5: f: PPy/LBM 10

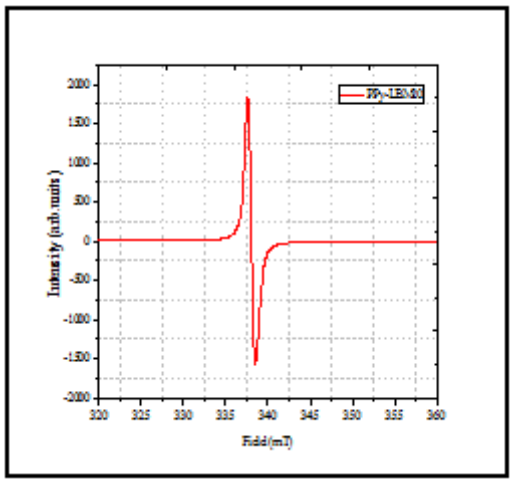

g: PPy/LBM 20

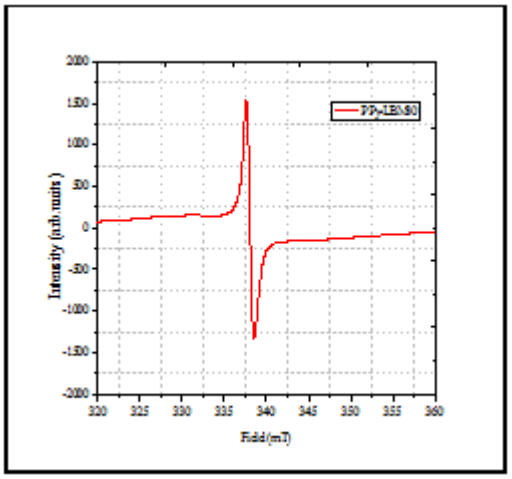

h: PPy/LBM 30

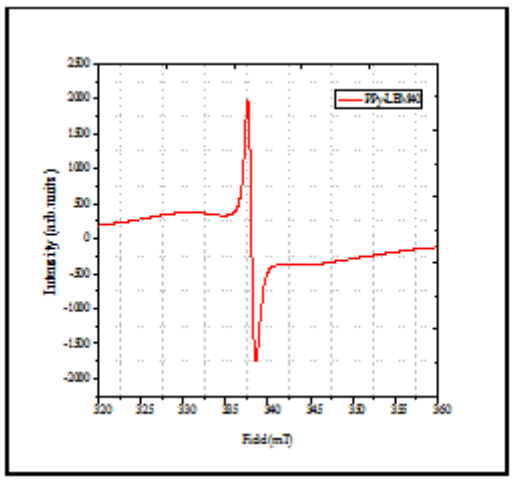

i: PPy/LBM 40

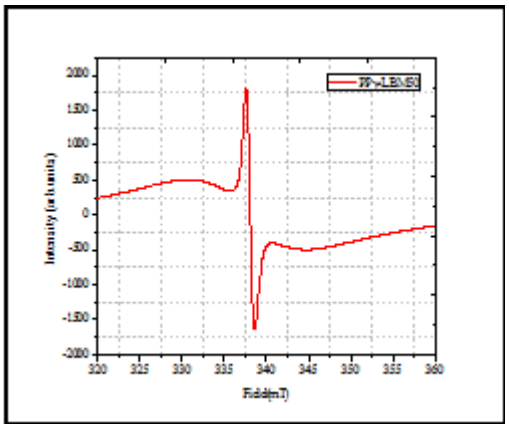

j: PPy/LBM 50

Table 2: Variation of G-Value and the Transition Responsible for the Behavior of the Samples

Name of the Compound	G-Value	Transition
PPy/LCM10	1.997	Mn^{4+}
PPy/LCM20	1.99	Mn^{4+}
PPy/LCM30	1.95	Mn^{4+}
PPy/LCM40	1.91	Mn^{4+}
PPy/LCM50	1.90	Mn^{4+}
PPy/LBM10	1.98	Mn^{4+}
PPy/LBM20	1.95	Mn^{4+}
PPy/LBM30	1.9	Mn^{4+}
PPy/LBM40	1.89	Mn^{4+}
PPy/LBM50	1.86	Mn^{4+}

The EPR plots of PPy/LCM and PPy/LBM nanocomposites are displayed in Figure 5. (a-e) and Figure 5. (f-j) respectively. In the case of the EPR spectra of PPy/LCM nano compounds, it's evident that the spectrum width diminishes as the LCM composition within the PPy chain increases. This trend is attributed to the favored reduction of spin which is responsible for the variation in the width at the deprotonation state **[25-27]**. Within the spectrum, both broad and narrow lines observed is due to delocalized and localized charge carriers, respectively, existing in ordered and disordered regions of the sample. This explanation aligns with the listed g values for the compounds. Notably, the observed decrease in g values is attributed to the amplification of anisotropy energy, a result of the interaction between the orbital motions of electrons at the interface with the doped material **[28-36].**

A common factor among all the compounds is the primary transitions resulting from the Mn4+ state.

V. CONCLUSION

We have synthesized a new type of composite material PPy/LCM and PPy/LBM nano composites by in situ oxidation method. The morphology, and crystalline phase were examined and showed that the particles are formed as expected. The magnetic properties studies using the VSM tool showed paramagnetic behavior for both PPy/LCM and PPy/LBM nanocomposites. The EPR studies confirmed the interaction between the host and the doped elements (LCM and LBM). This is for first time room temperature magnetic response study is been conducted. Further work will be conducted for SQUID applications.

REFERENCES

[1] Shirakawa, H,Louis, E. J, Macdiarmid, A. G,Chiang, C. K, Heeger, A. J**.** " Synthesis of electrically conducting organic polymers: halogen derivatives of polyacetylene, $(CH)_x$" J. Chem. Soc., Chem. Commun, 16, 578-580 , 1977.

[2] Matthew C Henry, Chen-Chan Hsueh, Brian P Timko, Michael S Freund, " Reaction of pyrrole and chlorauric acid a new route to composite colloids", J. Electro chem. Soc, 148, 11, 155-162, 2001.

[3] Bolto B.A, McNeill, R., Weiss, D.E. "Electronic Conduction in Polymers. III. Electronic Properties of Polypyrrole", Aust J Chem, 16, 6, 1090-1103, 1963.

[4] Om Prakash, Alka Mungray, Shobhana Chongdar, Suresh Kumar Kailasa, Arvind Kumar Mungray. Performance of Polypyrrole coated metal oxide composite electrodes for benthic microbial fuel cell. J. Environ.Chem.Eng 2020:8 (2):102757.

[5] Qi Wei and Zhijun Ning**.** Chiral Perovskite Spin-Optoelectronics and Spintronics: Toward Judicious Design and Application. ACS Materials Lett 2021:3 (9): 1266–1275.

[6] Sarkar, Kamanashis & Debnath, Ajit & Deb, Krishna & Bera, Arun & Saha, Biswajit. Effect of NiO incorporation in charge transport of polyaniline: Improved polymer-based thermoelectric generator, Energy 2019:177(C):203-210.

[7] Koshy, J, Kurian, J, Jose, R, John, A.M, Sajith, P.K.James, J.Pai, S.P. Pinto, R, "Novel ceramic substrates for high Tc superconductors", Bull. Mater Sci, 22, 3, 243-249, 1999.

[8] C wik, M. Lorenz, T. Baier, J. Muller, R. Andre G, Bour, F.Lichtenberg, F. Freimuth, A Schmitz, R.Hartmann, E. M. Braden M, "Crystal and magnetic structure of LaTiO3: Evidence for non degenerate t_{2g} orbitals", Phys. Rev. B, 68, 060401(R), 2003.

[9] B. Dabrowski, O. Chmaissem, J. Mais, S. Kolesnik, J.D. Jorgensen, and S. Short "Tolerance Factor Rules for $Sr_{1-x-y}Ca_xBa_yMnO_3$ Perovskites", J. Solid State Chem, 170, 1,154-164, 2002.

[10] P. Norby, I. G. Krogh Andersen, and E. Krogh Andersen, "The crystal structure of lanthanum manganite (iii), $LaMnO_3$, at room temperature and at 1273 K under N_2", J. Solid State Chem, 119, 191-196, 1995.

[11] C. Zener, "Interaction between the d Shells in the Transition Metals", Phys Rev, 81, 440,1951.

[12] Sacchidanand S. Shinde, Jayant A.Kher,Milind V.Kulkarni, "Synthesis, Characterization and Electrical Property of Silver Doped Polypyrrole Nanocomposites", Int. j. innov. res. sci. eng. technol, 3,ISSN: 2319-8753,2014.

[13] S.K. Singh, S.B. Palmer, D. Mck Paul, M.R. Lees, "Growth, transport, and magnetic properties of Pr0.67Ca0.33MnO3 thin films", Appl. Phys. Lett. 69, 263, 1996.

[14] E.L. Wolf, Nanophysics and Nanotechnology, (Wiley-VCH Verlag GmbH & Co., Weinheim, 2004.

[15] B.M Nagabhushanaa, G.T. Chandrappaa, R.P. Sreekanth Chakradharb, K.P. Rameshb, C. Shivakumarac, "Synthesis, structural and transport properties of Nanocrystalline $La_1K_xBa_xMnO_3$ (0.0%x%0.3) powders", Solid State Commun,136,7, 427-432,2005

[16] N. Naveen Kumar, S. Bastola, R. Kumar, Ranjan, 'Relaxor dielectric behavior in $BaTiO_3$ substituted $BiFeO_3$–$PbTiO_3$ multiferroic system', J. Mater. Sci, 28,14, 10420–10426,2017.
[17] B. Kurniawan, S. Winarsih, C. Kurniawan, M. R. Ramadhan, and F. Ruli, 'The effect of Ca-doping on structure and microstructure of $La_{0.7}(Ba_{1-x}Ca_x)_{0.3}MnO_3$', AIP Conference Proceedings, 1862, 03005, 2017.
[18] M. Baazaoui, S. Zemni, M. Boudard, H. Rahmouni, A. Gasmi, A. Selmi, M. Oumezzine, "Magnetic and electrical behavior of $La_{0.67}Ba_{0.33}Mn_{1-x}FexO_3$ perovskites", IJNeaM , 3, 23-36, 2010.
[19] N. Kallel, S. Ben Abdelkhalek, S. Kallel, O. Peña, M. Oumezzine, "Structural and magnetic properties of $(La_{0.7}0_{1-x}Y_x)$ $Ba_{0.3}Mn_{1-x}Fe_xO_3$ perovskites simultaneously doped on A and B sites ($0.0 \leq x \leq 0.30$", J.Alloys.Compd, 501, 30-36, 2010.
[20] Ma.Oumezzine, S. Zemni, O. Peña, "Room temperature magnetic and magneto caloric properties of $La_{0.67}Ba_{0.33}Mn_{0.98}Ti_{0.02}O_3$ perovskite", J.Alloys.Compd, 508,292-296, 2010.
[21] B.E. Warren, "X-ray Diffraction", Addison-Wesley, Massachusetts, 1969.
[22] B.D. Cullity, C.D. Graham, "Introduction to magnetic materials", 2nd ED., John Wiley & Sons, Hoboken, NJ, 2011.
[23] R. Grössinger, "A critical examination of the law of approach to saturation I. fit procedure", Phys Status Solidi A**,** 66, 665-674, 1981.
[24] I. Radelytskyi, P. Dłużewski, V. Dyakonov, P. Aleshkevych, W. Kowalski, P. Jarocki, H. Szymczak, "Magnetic anisotropy of $La_{0.7}Sr_{0.3}MnO_3$ nanopowders", J Magn Magn mater. , 335, 11-16,2013.
[25] Ignacio Muñoz Resta, José M. Sellés, Matías Lanús-Méndez-Elizalde, Paula S. Antonel, Fernando V. Molina, "Polypyrrole-$CoFe_2O_4$ nanocomposites: Polymer influence on magnetic behavior and particle effects on polymer conduction", Polym Composite**,** *39*, 12, 4617- 4627, 2018.
[26] Gyanti Prakash Moharana, Rahul Kothari, "Role of spin, phonon and plasmon dynamics on ferromagnetism in Cr doped 3C-SiC", J. Magn. Magn. Mater, 491, 1, 165505, 2019.
[27] Suresh Kumar Gupta, Vandna luthra, Ramadhar Singh, **"**Electrical transport and EPR investigations: A comparative study for d.c. conduction mechanism in mono valent and multivalent ions doped polyaniline", Bull. Mater. Sci., 35, 5,787–794, 2012.
[28] Ruma Gupta, Kavitha Jayachandran, J. S. Gamare, B. Rajeshwari, Santosh K. Gupta, J. V. Kamat, "Novel Electrochemical Synthesis of Polypyrrole/Ag Nanocomposite and Its Electrocatalytic Performance towards Hydrogen Peroxide Reduction", J. Nanomater, 1-6, 2015.
[29] Till Biskup, "Structure–Function Relationship of Organic Semiconductors: Detailed Insights From Time-Resolved EPR Spectroscopy", Front Chem,7,2019.
[30] Manahil E. Mofdal1, Batool Eneaze Al-jumaili, Zainal A. Talib, Ibrahim Bagudo Muh'd, Mubarak tagbo1, "The evaluation of Temperature effect on Peak-to- Peak Line Width (ΔHpp) of conjugating polymer Polypyrrole (Ppy)", J. Phys. Conf. Ser. 1178 01,2021.
[31] Yunze Long,Zhaojia Chen,Jiaoyan Shen,Zhiming Zhang,Lijuan Zhang, Hongmei Xiao,Meixiang Wan,Jean Luc Duvail, "Magnetic Properties of Conducting Polymer Nanostructures", J. Phys. Chem. B,110, 46, 23228-23233, 2006.
[32] Jiang Guo, Hongbo Gu, Huige Wei,Qianyi Zhang, Neel Haldolaarachchige, Ying Li,David P. Young, Suying Wei, Zhanhu Guo, "Magnetite−Polypyrrole Meta composites: Dielectric Properties and Magneto resistance Behavior", J. Phys. Chem. C 117, 10191−10202, 2013.
[33] P Poddar, J LWilson, H Srikanth, S.A.Morrison, E E Carpenter, "Magnetic properties of conducting polymer doped with manganese–zinc ferrite nanoparticles", Nanotechnology, 15, 570–574, 2004.
[34] T. Bashira,c, A. Shakoora, E. Ahmeda, N. A. Niaza, Shahid Iqbald,Muhammad Saeed Akhtarb, Mohammad Azad Malik, "Magnetic, Electrical and Thermal Studies of Polypyrrole-Fe2O3 Nanocomposites", Polym. Sci. Ser. B, 59, 6, 902–908, 2017.
[35] V. Sitaram, Ajay Sharma, S. V. Bhat, K. Mizoguchi, and Reghu Menon, "Electron spin resonance studies in the doped polyaniline PANI-AMPSA: Evidence for local ordering from line width features", Phys. Rev. B 72, 035209, 2005.
[36] D. D. Ateh1,H. A. Navsaria, P. Vadgama1, "Polypyrrole-based conducting polymers and interactions with biological tissues", J. R. Soc. Interface, 3, 11,741–752, 2006.

